Science of the Total Environment 957 (2024) 177525

Contents lists available at ScienceDirect

Science of the Total Environment

journal homepage: www.elsevier.com/locate/scitotenv

Remote sensing and spatial analysis reveal unprecedented cyanobacteria bloom dynamics associated with elephant mass mortality

Davide Lomeo [a,*], Emma J. Tebbs [a], Nlingisisi D. Babayani [b], Michael A. Chadwick [a], Mangaliso J. Gondwe [b], Anne D. Jungblut [c], Graham P. McCulloch [d], Eric R. Morgan [e], Daniel N. Schillereff [a], Stefan G.H. Simis [f], Anna C. Songhurst [d]

[a] Department of Geography, King's College London, London, United Kingdom
[b] Okavango Research Institute, University of Botswana, Maun, Botswana
[c] Department of Life Sciences, Natural History Museum, London, United Kingdom
[d] Ecoexist, Maun, Botswana
[e] School of Biological Sciences, Queen's University, Belfast, United Kingdom
[f] Plymouth Marine Laboratory, Plymouth, United Kingdom

HIGHLIGHTS

- Elephant carcasses clustered near waterholes (pans) with high algal biomass in 2020.
- 20 pans showed unprecedented bloom events during the mass mortality period.
- Elephants may have travelled 16.5 km and died within 88 h of toxin exposure.
- Shift from dry 2019 to wet 2020 likely triggered extreme algal growth in pans.
- Spatial analysis and remote sensing provide new framework for mortality studies.

GRAPHICAL ABSTRACT

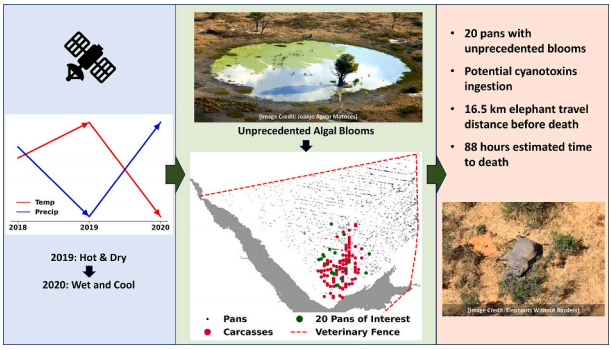

ARTICLE INFO

Editor: Rafael Mateo

Keywords:
Cyanobacteria
Mass mortality event
Spatial analysis
Remote sensing
Eco-hydrology
Water quality
Monitoring

ABSTRACT

The 2020 mass mortality of 350 African elephants (*Loxodonta africana*) in Botswana sparked global concern, with cyanotoxins in watering holes (pans) being a suspected cause, though evidence remains inconclusive. Combining remote sensing and spatial analysis, we examined the relationship between the ecohydrology of ~3000 pans and the locations of deceased elephants. Our analysis revealed a significant difference in the spatial distribution of fresh versus decayed carcasses ($p < 0.001$), indicating that the die-off deviated from typical regional elephant mortality patterns. We identified 20 pans near fresh carcasses that experienced increased cyanobacteria bloom events in 2020 ($n = 123$) compared to the previous 3 years combined ($n = 23$), exhibiting the highest average phytoplankton biomass of the period 2015–2023 (Normalised Difference Chlorophyll Index >0.2). These findings suggest a heightened risk and likelihood of cyanotoxin presence in these pans. Elephants were estimated to have

* Corresponding author.
E-mail addresses: davide.lomeo@kcl.ac.uk (D. Lomeo), emma.tebbs@kcl.ac.uk (E.J. Tebbs), NBabayani@ub.ac.bw (N.D. Babayani), michael.chadwick@kcl.ac.uk (M.A. Chadwick), mgondwe@UB.AC.BW (M.J. Gondwe), a.jungblut@nhm.ac.uk (A.D. Jungblut), Eric.Morgan@qub.ac.uk (E.R. Morgan), daniel.schillereff@kcl.ac.uk (D.N. Schillereff), stsi@pml.ac.uk (S.G.H. Simis), fielddirector@ecoexistproject.org (A.C. Songhurst).

https://doi.org/10.1016/j.scitotenv.2024.177525
Received 1 September 2024; Received in revised form 9 November 2024; Accepted 10 November 2024
Available online 16 November 2024

walked 16.5 km (± 6.2 km) and died within 88 h (± 33 h) of exposure. Our study provides evidence that cyanobacterial toxicity could be a contributing factor to the 2020 die-off, while also considering other potential causes, and offers a general framework for investigation of future mortality events. We underscore the need to integrate spatial analysis and regional ecohydrological assessments to monitor and mitigate animal mortality events and inform conservation strategies.

1. Introduction

The 2020 die-off of 350 elephants in Botswana was one of the biggest mortality events of large wild mammals in southern Africa in recent years (Barton et al., 2023). The remote location in the north-eastern sector of Botswana known as the eastern Okavango Panhandle, and timing at the peak of the COVID-19 pandemic, hindered attempts to respond to and investigate the event (Van Aarde et al., 2021). Although this area is a known poaching hotspot in Botswana (Pozo et al., 2017), this was ruled out since elephant carcasses were found with tusks intact (Maron, 2020). Other initial theories included virulent and bacterial causes, such as encephalomyocarditis virus or anthrax, but evidence from the field, such as the age of dead elephants, and the absence of clinical signs, deemed both unlikely (Azeem et al., 2020). The cause of the die-off has been officially attributed by the Government of Botswana to environmental intoxication by cyanobacterial toxins, also known as cyanotoxins (Benza, 2020).

Cyanobacteria are a group of benthic or planktonic phototrophic prokaryotes often abundant in turbid, stagnant, and nutrient-rich waters, and several bloom-forming species can cause harm due to the production of toxins (Merel et al., 2013; Huisman et al., 2018). Evidence suggests that phytoplankton (microalgae or cyanobacteria) blooms, events in which population size increases exponentially due to favourable conditions (Paerl and Otten, 2013), are becoming more frequent worldwide due to increased anthropogenic nutrient input and climate change (Hou et al., 2022). Links between harmful blooms and animal mortality events are well represented in literature, including cyanotoxin poisoning (Wood, 2016; Svirčev et al., 2019). Cyanobacteria are a common occurrence in water bodies in southern Africa (Matthews et al., 2010; Dalu and Wasserman, 2018; Feng et al., 2024), and have previously been linked to wildlife mortality events (Bengis et al., 2016).

An Investigation on the 2020 elephant die-off event supported cyanotoxins as the likely cause, showing that hypereutrophic waters in southern Africa pose exceptionally high risks of cyanotoxin exposure to wildlife, with climate extremes potentially triggering both this and prehistoric mass mortality events (Wang et al., 2021). This is further supported by a comprehensive meta-analysis revealing that cyanotoxin concentrations in African inland waters are often found thousands of times higher than WHO guidelines, with particularly high levels in smaller waterbodies in southern Africa (Zhao et al., 2023).

The Okavango Delta is hydrologically complex and characterised by permanent and ephemeral waterbodies filled by seasonal flooding or local rainfall alongside the river itself and associated lakes. Evidence of increased cyanobacteria bloom occurrences in perennial lakes within the Okavango Delta in 2020 reinforced the possibility of cyanotoxin involvement (Veerman et al., 2022), with subsequent work revealing how drought conditions likely drove these exceptional blooms (Veerman et al., 2024). However, new evidence of *Pasteurella* sp. in carcasses arisen from a die-off event of elephants in the neighbouring Zimbabwe in 2020, suggest that this bacterium may have been the cause of the mass mortality event in Botswana (Foggin et al., 2023). Unfortunately, as the event occurred in an especially remote location hard to sample logistically, during enforced movement restrictions, comprehensive in situ water and tissue samples contemporary with the die-off have not been collected. Moreover, the state of waterholes (or pans) in the eastern Okavango Panhandle, directly where the die-off occurred, has never been assessed, which would elucidate on the possibility of cyanobacteria involvement in the die-off.

In the absence of solid outbreak sample data, we explore an alternative strategy to reconstruct elephants' travel ranges in relation to the distribution and eco-hydrology of pans in the eastern Okavango Panhandle. This study implements an extensive spatial analysis, integrating the distribution of elephant carcasses documented during a post-mortality aerial survey (Songhurst and Tsholofelo, 2020), and satellite-derived data on the location and condition of regional pans. In particular, the Automated Water Extraction Index (AWEI) (Feyisa et al., 2014) was used to indicate the location and water availability of pans, while the Normalised Difference Chlorophyll Index (NDCI) (Mishra and Mishra, 2012) was used as a proxy for phytoplankton biomass in pan water. The generic NDCI is used as an indicator of biomass concentrations because other diagnostic alternatives that provide concentration estimates in mg m^{-3} do not exist for such small and shallow waterbodies. Noting that cyanotoxins are not directly detectable from space, the presence and abundance of cyanobacteria, especially if bloom-forming - known to be dominant in regional pans (Hart, 1997; Msiteli-Shumba et al., 2018) - can increase the likelihood of cyanotoxin production and accumulation.

The integration of spatial analysis, remote sensing, and eco-hydrological assessment not only circumvents logistical challenges but also provides a scalable model for investigating wildlife mortality events in similarly inaccessible regions, where traditional field-based methods may be impractical or impossible. This work addresses a crucial gap in understanding the spatial-temporal relationship between pan conditions and elephant deaths. We investigate whether the proximity of carcasses to pans with suspected phytoplankton bloom activity corroborates the hypothesis that deteriorating water quality has caused the die-off. Our results contribute to elucidating the causes behind such mass mortality events and demonstrate the utility of incorporating spatial analysis and remote sensing into routine wildlife health and water quality monitoring globally. This approach enhances wildlife conservation efforts and informs public health strategies, providing vital insights for potentially preventing and controlling future incidents.

2. Material and methods

2.1. Study area

The study focused on the eastern Okavango Panhandle region, the north-easternmost sector of the Okavango Delta, directly where the elephant mass mortality event occurred, which comprises the concession areas NG11, NG12 and NG13 within the Ngamiland district, Botswana (Fig. 1). The area is enclosed by veterinary fences to the north (a double border fence with Namibia) and a 'buffalo fence' to the east and south. These fences were originally installed to prevent the transmission of zoonotic diseases from wild animals to domestic animals, like the foot and mouth disease carried by buffalos (Perkins, 2019), and the Contagious Bovine Pleuropneumonia (CBPP) (Marobela-Raborokgwe, 2011). The west side of the eastern Okavango Panhandle is closed-off by the Okavango River where the water is relatively deeper and prevents non-aquatic animals from routinely crossing to either side (Van Aarde et al., 2021). The total extent of NG11, NG12 and NG13 concession areas within the veterinary fence and including the Okavango River is ~9300 km^2.

The climate of Botswana is classified as arid to semi-arid, and as such it is characterised by two distinct seasons. The wet season occurs between November and March, when total rainfall range between 300 mm

and 600 mm per year. During the dry season between April and October, rainfall is virtually absent. Temperatures average between 15 °C and 27 °C, with peak low temperatures below 0 °C at night in winter (June to August), and peak high temperatures of over 40 °C during the day in summer (November to February) (Byakatonda et al., 2018; Nkemelang et al., 2018; Akinyemi and Abiodun, 2019).

The elephant population in Botswana is currently the largest on Earth, counting over 132,000 individuals as of the latest report from the KAZA TFCA aerial survey (Bussière and Potgieter, 2023). The most updated published record of wildlife populations within the eastern Okavango Panhandle is from a dry season survey conducted in 2018, where over 15,000 elephants were estimated, alongside 25,000 cattle, 5000 zebras, 4500 goats and 500 wildebeest, to mention the most abundant animals (Chase et al., 2018). Population estimates from past and current surveys in the Panhandle, however, show large fluctuations, but the trend has shown that the population has been increasing at around 9.5 % a year (Songhurst et al., 2015). Reasons for such high population increases is unknown but could be due to high immigration and low emigration from and to other areas, population structure and recruitment rates, or climatic conditions such as response to droughts.

2.2. Datasets

2.2.1. Elephant survey data

The location of elephant carcasses and live animals was obtained from an aerial survey of the eastern Okavango Panhandle conducted by the Department of Wildlife and National Parks (DWNP) of Botswana and Ecoexist (Ecoexist, 2023) in July 2020 (Songhurst and Tsholofelo, 2020). This survey was the first official investigation conducted on the mortality event following the first elephant deaths reported by local rangers on the 18th of March 2020 (African News Agency, 2020). The aerial survey, which employed the standard methodology of strip transect sampling (Norton-Griffiths, 1978), aimed to count the number of carcasses and live animals and estimate the age category of the carcasses. The survey used a standard classification method to estimate the age of the carcasses (Douglas-Hamilton and Burrill, 1991) but adjusted based on local knowledge of carcasses decay in the region. The survey classified carcasses aged <1 month as fresh (C1) (i.e., deaths occurred between June and July 2020), carcasses aged >1 month and < 6 months as recent (C2) (i.e., deaths occurred in the period Jan-Jun 2020), and those aged >6 months as bones (Songhurst and Tsholofelo, 2020). In this work we combined carcasses estimated from their state of decomposition as C1 and C2 into a single category named *carcasses* due to the limited number of C1 points available. The other two categories obtained from the survey were *bones* and *live elephants*. Bones were used as an indication of what a 'normal' or 'natural' distribution of carcasses across the eastern Okavango Panhandle is expected to be, whereas carcasses with skin were assumed to be very recent thus associated with the die-off event.

2.2.2. Climate and remote sensing data

Air temperature 2 m above ground between 2015 and 2023 was obtained from the ERA5 hourly re-analysis dataset provided by the European Centre for Medium-Range Weather Forecasts (ECMWF) at a

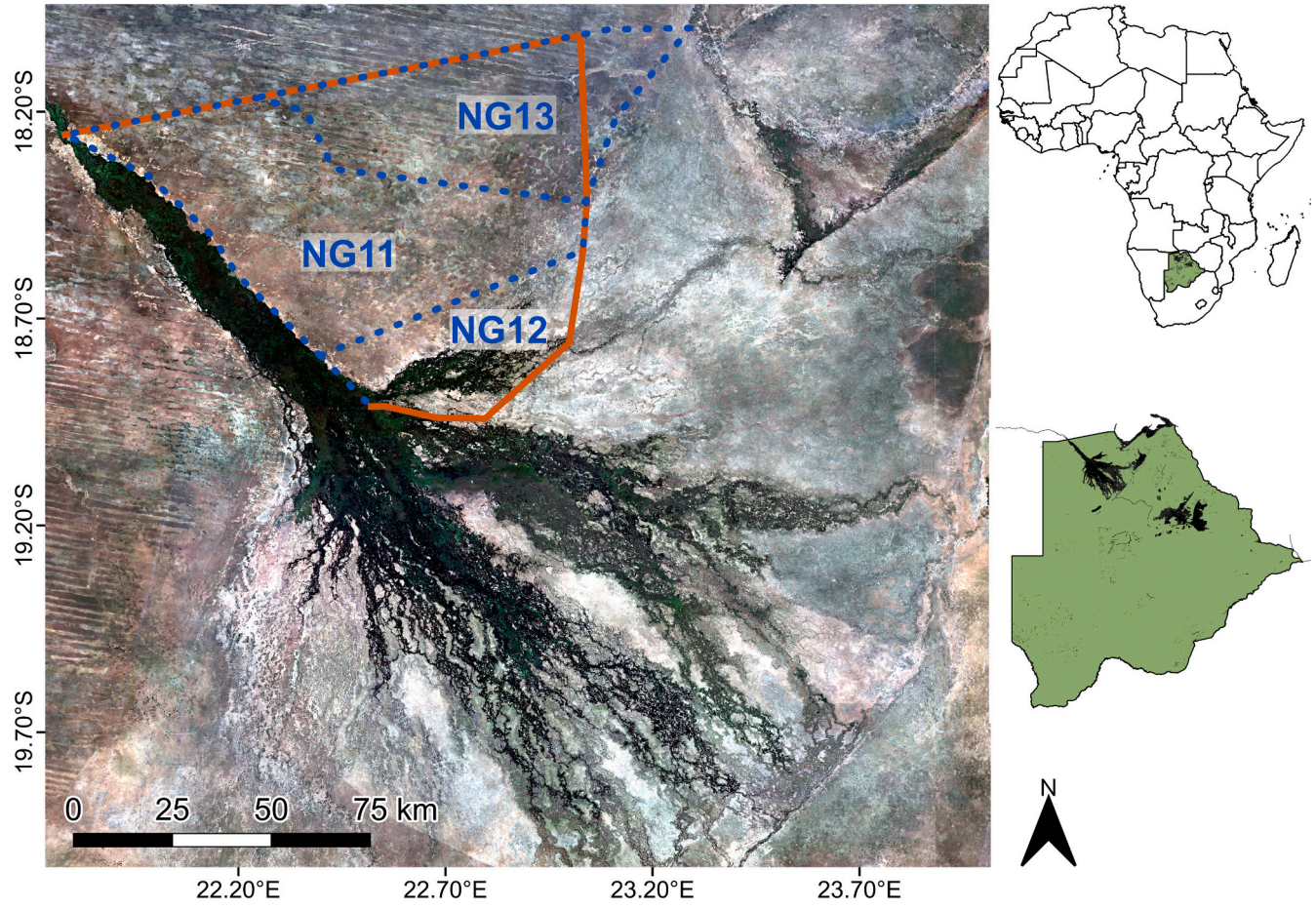

Fig. 1. The panel on the left shows an image composite of the Okavango Delta, located in the north of Botswana, captured by Sentinel-2 Multispectral Instrument-A (Level 2 A) in the period 15–31/05/2020. The blue dotted lines are the boundaries of the concession areas NG11, NG12 and NG13. The orange lines show the boundaries of the veterinary fence that runs along the border with Namibia in the north. The green shape to the right shows the territory of Botswana, and the black areas within it are areas where water is regularly detected.

resolution of 0.25° (~25km^2) (Hersbach et al., 2023). Precipitation data was obtained from the TAMSAT dataset between 2015 and 2023, which comprises rainfall estimates based on satellite and ground-based observations for the African continent at 0.0375° resolution (~4 km^2) (Maidment et al., 2014; Tarnavsky et al., 2014; Maidment et al., 2017).

Sentinel-2 Multispectral Instrument (MSI)-A/B Level-2 A images (i.e., atmospherically, and geometrically corrected) between January 2019 and August 2023 were obtained from Google Earth Engine (GEE). These were filtered by cloud cover (60 %). Pixels were scanned through the *s2cloudless* algorithm (Braaten, 2023) and masked if holding a probability >50 % of being affected by cloud or cloud shadow. Since images prior 2019 were not available on GEE as Level-2 A, individual cloud-free MSI-A/B Level-1C images between 2015 and 2018 were downloaded from CREODIAS data explorer online tool (CREODIAS, 2023). These were filtered for clouds and atmospherically corrected using the European Space Agency's (ESA) default *Sen2Cor* atmospheric correction algorithm (ESA, 2020a, 2020b).

2.3. Identification of pans

A water frequency product developed for the Kavango-Zambezi Transfrontier Conservation Area (KAZA) for the period 2017–2020 (Swift et al., 2022) was used to provide a general location of pans the eastern Okavango Panhandle. The product was cropped to the extent of the veterinary fence within the region (Fig. 1), resulting in a total area of 7138 km^2. The Okavango River and its north-eastern branching were removed to enhance the identification of individual pans, explained in more details below. The cropped water frequency product was vectorised using QGIS Białowieża LTR v3.28.11, providing a series of individual polygons, each representing the estimated area of the pans in the region.

The Automated Water Extraction Index (AWEI) (Feyisa et al., 2014) was calculated from MSI-A/B images to distinguish between land and water pixels within the target polygons using the equation:

$$AWEI = \rho_{B2} + 2.5 \times \rho_{B3} - 1.5 \times (\rho_{B8} + \rho_{B11}) - 0.25 \times \rho_{B12}) \quad (1)$$

where ρ_{Bn} are Sentinel-2 MSI bands blue (B2, 490 nm), green (B3, 560 nm), NIR (B8, 705 nm), SWIR1 (B11, 1610 nm) and SWIR2 (B12, 2190 nm), respectively. Although negative AWEI values are typically associated to land pixels, AWEI <0 can sometimes be associated to water (Schaffer-Smith et al., 2022). This is because very small and highly turbid waterbodies can be spectrally similar to land (except at longer wavelengths).

The Grey Histogram algorithm (Otsu, 1979) was computed to identify an optimal AWEI threshold from the 95th percentile values in images between Mar and May of each year to distinguish between pan turbid water and land. The 95th percentile was used to capture water at its maximum extent (i.e., at the transition from wet to dry season) while minimising false positives (undetected cloud pixels) and false negatives (adjacent land effect). The removal of the Okavango River and associated wetlands from the water frequency product was necessary to account for the significant spectral difference between the clearer water of the river system, which exhibited positive AWEI values, and the turbid water in pans, which largely exhibited negative AWEI values. AWEI thresholds were averaged to account for potential biases typically introduced by atmospheric correction algorithms, obtaining a value of AWEI = −0.3624 (rounded). The threshold was applied to all the images between 2015 and 2023, and each group of contiguous pixels within each polygon was considered an individual pan.

Bi-weekly 95th percentile values were calculated from consecutive images for two periods each month: from the 1st to the 15th, and from the 15th to the last day. This approach ensured temporal continuity of measurements and mitigated data gaps resulting from cloud filtering, masking, and the occasional absence of MSI images. The area of individual pans was estimated by counting contiguous pixels within each delineated polygon. Pan locations were tracked using the latitude and longitude coordinates of polygon centroids. At these centroid locations, both the AWEI, used as a proxy of water availability, and the Normalised Difference Chlorophyll Index (NDCI) (Mishra and Mishra, 2012), used as an indicator of phytoplankton biomass, were extracted. NDCI was obtained with the equation:

$$NDCI = \frac{\rho_{B5} - \rho_{B4}}{\rho_{B5} + \rho_{B4}} \quad (2)$$

where ρ_{Bn} are Sentinel-2 MSI bands near-infrared (B5, 705 nm) and red (B4, 665 nm), respectively. This index provides values in the range −1 to 1. Positive values are associated to surface phytoplankton biomass.

The final collated dataset encompassed 128,667 pan observations between 2015 and 2023, with individual pans being recorded multiple times due to the bi-weekly sampling frequency. The month exhibiting the maximum cumulative pan area (i.e., greatest water extent - April 2021) was used to identify distinct pans. This approach yielded a total of 3389 individual pans. Acknowledging that pan centroids were likely to shift as water levels fluctuated over time, a 30-m tolerance radius around each centroid was implemented to maintain consistent labelling of individual pans across the temporal dataset.

2.4. Location comparison between surveyed live and dead elephants

The Nearest Neighbour (NN) distance (Clark and Evans, 1954) was used to evaluate if the distribution of carcasses differed from that of bones and live elephants, using the equation:

$$\mathrm{NN} = \frac{\overline{D}}{E[D]}; \quad (3)$$

Where: $E[D] = \frac{1}{2\sqrt{\lambda}}$; $\lambda = \frac{n}{A}$

Here, $\overline{D}$ is the average distance across all pairs of points and $E[D]$ is a random distribution of points given λ, which is the point density (n is the number of points, A is the area). The significance of the NN distance was evaluated using a Monte Carlo simulation, which randomly permuted the locations of datapoints within the region to simulate complete spatial randomness (Kroese et al., 2014). The Monte Carlo simulation was run for 999 iterations, ensuring both statistical robustness and computational efficiency. For each iteration, the NN was calculated for the simulated randomly distributed set of points and compared to the observed points using a z-score, which assessed the degree to which the spatial pattern of the observed points deviated from a random distribution. The z-score was obtained with the formula:

$$\mathrm{Z} = \frac{\overline{D} - E[D]}{SE} \quad (4)$$

where SE is the standard error of the mean distance in a random distribution. A z-score outside the range of −1.96 to 1.96 indicates the presence of statistically significant clustering or dispersion at the 95 % confidence level. The points for each elephant category (carcasses, bones, and live elephants) were cross-compared to determine if their distributions differed statistically using the non-parametric two-sample Kolmogorov-Smirnov (KS) test, which uses every point in the samples irrespective of distribution and ordering (Massey, 1951; Lopes et al., 2007).

2.5. Clusters identification

The number of clusters generated by each category based on inter-point distances was determined to further assess the spatial distribution patterns of carcasses, bones, and live elephants across the landscape. The number of clusters in each category provided an indication of spatial associations between points, with fewer clusters potentially denoting a higher likelihood of relationship between points. Cluster

identification was performed using the Density-Based Spatial Clustering of Applications with Noise (DBSCAN) method (Ester et al., 1996), a density-based algorithm that identifies distance-based clusters within groups. DBSCAN uses an optimal average distance, referred to as epsilon, and a minimum number of points to generate clusters. The epsilon value was automatically derived from the data using an 'elbow method' algorithm. This approach sorted inter-point distances in ascending order and employed a moving average to identify the optimal value as the point at which distances increased sharply. The minimum number of points was set to 4 to prevent the formation of excessively small clusters.

2.6. Point pattern analysis

The spatial autocorrelation between pan locations and the centre of each elephant category was calculated to determine which pans elephants may have interacted with most frequently before dying. Cluster centres were preferred over individual points to mitigate noise from randomly distributed points and to delineate areas common to spatially associated groups of carcasses and bones. The Local Moran's I statistic (Anselin, 1995) was employed to assess spatial autocorrelation and measure the similarity between neighbouring pans based on their proximity to cluster centres. Given a set of n spatial units (i.e., the total number of pans for a given timestamp), and a variable x observed over these units (i.e., the distance between individual pans and the clusters centres), the Local Moran's I for the i-th unit (individual pan) was defined as:

$$I_i = \frac{(n-1)(x_i - \bar{x})\sum_j w_{ij}(x_j - \bar{x})}{\sum_i (x_i - \bar{x})^2} \quad (5)$$

Where x_i and x_j are the distances of pans i and j to the nearest cluster centre, $\bar{x}$ is the mean distance across all pans, w_{ij} is the spatial weight, indicating whether j is neighbour of pan i, and n is the total number of pans. The denominator serves as a normalisation factor, representing the global variance of pan-cluster centres distance. The spatial weights matrix was computed by applying a k-Nearest Neighbours (k−NN) algorithm to the pan locations. The optimal k was dynamically calculated as the number of pans within twice the average distance between all pans (Anselin, 1995) to avoid potential biases that might occur when setting a fixed k for areas of varying point density.

2.7. Reported animal intoxication

Due to the lack of literature specific to elephants, the potential distance travelled by elephants between initial exposure to cyanotoxins and death was estimated using known time-to-death in various animals following cyanotoxin exposure. The primary source of this information was the supplementary material in Wood (2016), which provides an extensive compilation of observations from published scientific literature spanning from 1878 to 2012. In some instances the causal link between cyanobacteria ingestion and death was circumstantial rather than definitively proven through laboratory assessment. However, these cases were supported by complementary empirical evidence, such as observations of animal deaths following interaction with water surfaces covered in green or blue-green substances. Only the observations with relatively specific timeframes of death we included to ensure precision in the analysis. Descriptions such as 'death within days' or 'died shortly after' were excluded due to their lack of temporal specificity. Conversely, more precise timeframes were retained and quantified as follows: 'minutes' was assigned a value of 30 min, 'few hours' was interpreted as 6 h, and 'several hours' was estimated at 12 h. This approach allowed to establish a more quantitative basis for estimating potential travel distances.

2.8. Standard deviation ellipses

Standard Deviation Ellipses (SDE) were computed for each carcass cluster centre to identify their bivariate latitude-longitude distribution and express their dispersion and orientation (Wang et al., 2015). The SDE method allowed for the identification of areas where elephants were likely to have interacted, taking into account the spatial arrangement of carcasses across the landscape. This approach aligns with the understanding that elephants do not move in a single direction throughout the day (Loarie et al., 2009). The SDE was calculated using the adapted ellipse equation:

$$\frac{(x-h)^2}{(p^*\sigma_x)^2} + \frac{(y-k)^2}{(p^*\sigma_y)^2} = 1 \quad (6)$$

where: $h = \frac{1}{n}\sum_{i=1}^{n} x_i; k = \frac{1}{n}\sum_{i=1}^{n} y_i;$

and: $\sigma_x = \sqrt{\frac{1}{n}\sum_{i=1}^{n}(x_i - h)^2}; \sigma_y = \sqrt{\frac{1}{n}\sum_{i=1}^{n}(y_i - k)^2};$

Here, n is the total number of points, x_i and y_i are the x and y coordinates of each point, respectively, h and k are the x and y coordinates of the mean points centre, respectively. The factor p determined the number of standard deviations to consider when computing the width and height of the ellipse.

3. Results

3.1. Spatial analysis of elephant carcasses and live elephants

The aerial survey carried out in mid-July 2020 to investigate the elephant mass mortality event counted 161 carcasses, 222 bones, and 2682 live elephants across the eastern Okavango Panhandle. The dead elephants were of varying age, with tusks intact, and no carcasses of other wildlife or livestock species were observed at the time of the survey. The spatial distribution of elephant carcasses significantly differed from that of bones and live elephants, suggesting that the mortality event affected specific areas rather than being uniformly distributed across the region (Table 1). The dissimilarity between carcass and bone distributions also indicates that this event created a spatial pattern distinct from historical mortality, pointing to localised factors potentially contributing to the die-off and warranting further investigation into specific environmental or ecological conditions in these areas.

Live elephants were primarily observed in dry woodlands, particularly in the NG11 and NG13 sectors of the eastern Okavango Panhandle, and dispersed across the NG12 area, near the Okavango Delta wetland system and along the 'buffalo' veterinary fence (Fig. 2). In contrast,

Table 1
Table of the Nearest Neighbour (NN) distance and the Two-sample Kolmogorov-Smirnov (KS) test. The NN shows how the points for each of the categories (bones, carcasses, live elephants) distribute across the region. NN close to 1 indicates random distribution, whereas NNI < 1 indicates clustering (stronger clustering approaching 0). The NN z-score shows the degree of clustering of each of the categories after comparison with randomly distributed points obtained with a Monte Carlo simulation. Large negative numbers indicate strong clustering. KS shows if the distributions of the paired categories are statistically different, with D statistic indicating their similarity. D close to 0 suggest that two samples are similar, D close to 1 indicates a large difference between samples.

Nearest Neighbour (NN) distance			Two-samples Kolmogorov-Smirnov Test		
Elephant Categories	NN	NN (z-score)	Elephant Categories pairs	*p*-value	D Statistic
Bones	0.769	−5.947	Bones - Carcasses	<0.001	0.24
Carcasses	0.532	−10.404	Bones - Live Elephants	<0.001	0.77
Live Elephants	0.029	−92.709	Live Elephants - Carcasses	<0.001	0.83

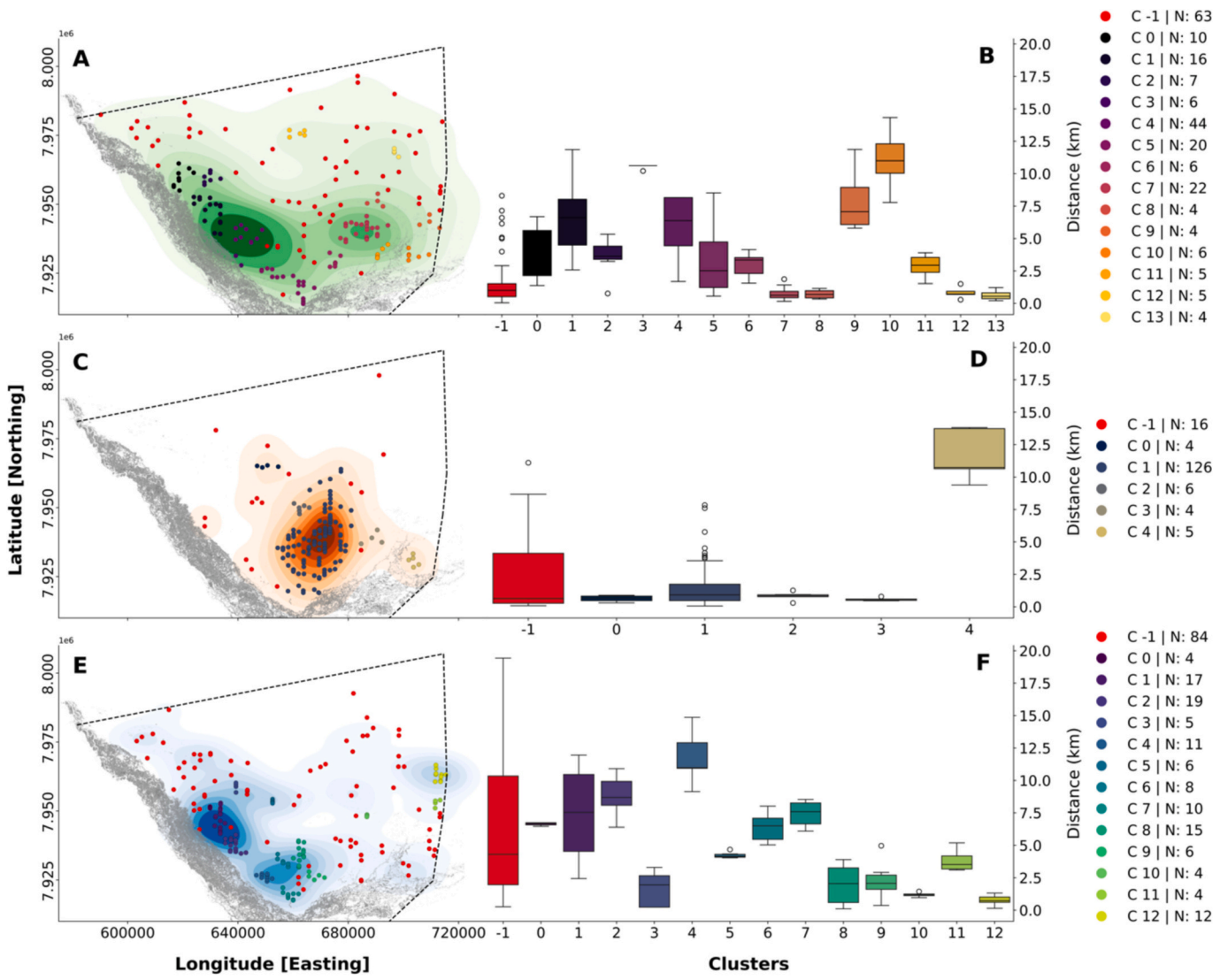

Fig. 2. Panels A, C and E show the distribution of bones, fresh carcasses, and live elephants across the eastern Okavango Panhandle, respectively. The shadings around the points represent the kernel density estimates of their distributions, and the weight of the colours are gradually more intense towards areas of higher concentrations of points. The dotted black lines represent the veterinary fence. Panels B, D and F show boxplots of distances between individual bones, carcasses, and live elephants belonging to different clusters and the nearest pan, respectively. For bones and carcasses, we used the location of pans detected by Sentinel-2 Multispectral Instrument (MSI)-A/B in April 2020 (i.e., peak of wet season in 2020). For live elephants we used the location of pans detected by MSI-A/B at the time of the aerial survey (July 2020). Clusters numbered as −1 and coloured in red in the maps and in the boxplots are not statistically significant points in the overall dispersion of the categories ($p > 0.05$). These points do not belong to any cluster and are not included in the analysis. The points in panels A, C, and E, are coloured such that they match the colour of the cluster they belong to in the boxplots in panels B, D and F, respectively. The legends to the right of the image refer to the panels in the same row, where 'C' refers to the cluster number, 'N' refers to the number of individuals belonging to each cluster.

bones were scattered more broadly across the landscape, covering an area of approximately 6500 km^2, with notable concentrations near the eastern Panhandle's wetlands. Carcasses were primarily found in a more confined area (~4350 km^2), considerably distant from the wetlands and human settlements. The analysis revealed significant differences in the proximity of each elephant category to water sources. Carcasses were, on average, located closer to pans (1635 m ± 2317 m) compared to bones (4545 m ± 3477 m) and live elephants (5672 m ± 3814 m). Distinct clustering patterns emerged among the categories. Live elephants exhibited the most pronounced clustering, followed by carcasses, then bones. This variance was statistically significant ($p < 0.001$, Table 1), highlighting different spatial behaviours and associations. Specifically, bones showed the greatest number of clusters ($n = 14$), indicative of widespread dispersion, followed by live elephants ($n = 13$), and carcasses ($n = 5$), with the average number of individuals per cluster substantially higher for carcasses ($n = 29 \pm 54$) than for bones ($n = 11 \pm 11$) or live elephants ($n = 9 \pm 5$). Notably, a significant portion of the carcasses were found within a single cluster ($n = 126$), hinting at a common underlying cause for these deaths.

3.2. Ecohydrology of pans and climate

The investigation of the ecohydrology of the 3389 pans in the eastern Okavango Panhandle revealed a major shift in water availability and phytoplankton growth between 2019 and 2020. This suggests potential implications for water quality, which may have impacted local wildlife. MSI-A/B imagery revealed a strong interannual fluctuations in the number of pans. The highest number of pans was observed in 2021 ($n = 3389$), while the lowest was recorded in 2016 ($n = 724$) (not considering 2015, for which image collection started from August). The Local Moran's I statistic allowed to identify a set of 1232 pans (from the maximum count in April 2021) spatially related to carcasses cluster centres ($p <$

0.05). NDCI in these pans exhibited consistently high values since 2020, contrasting with more variable pre-2020 levels (Fig. 3). AWEI values showed a dramatic increase in water availability from 2020, diverging from consistently low levels before 2019. Contextualising these findings against background environmental conditions, it was found that 2019 had one of the lowest precipitation levels in the period 2010–2023, followed by an extremely wet 2020. Temperature in 2019 was much higher than the 2010–2023 average and followed by a relatively cooler 2020. Pans in proximity to carcass cluster centres revealed that a marked increase in water availability coincided with sustained high phytoplankton biomass, as evidenced by post-2019 NDCI. The drastic changes in ecohydrological and climate conditions, particularly in the shift between 2019 (low rainfall and high temperatures) and 2020 (high rainfall and lower temperature), underscore the likelihood for altered water quality and increased harmful cyanobacteria bloom risks. These environmental dynamics, occurring in tandem with the carcass spatial clustering, provide compelling evidence of water quality deterioration as a possible contributing factor in the mass die-off event.

3.3. Distance covered by elephants before death

Toxicological timelines of cyanotoxin-related animal deaths in the literature – a complete list is available in Wood (2016) – suggested an association between animal size and time of death, the latter occurring between 15 min and 120 h after initial exposure (Table 2). Most of these studies focused on dogs, cattle, and sheep, with some instances of wildlife reporting like deer and rhinoceros. Extrapolating these findings to elephants, we looked at potential timeframes of 24, 48, 72, 96, 120, and 144 h (Fig. S1) to estimate distances covered by elephants between potential cyanotoxin exposure and death. These were converted to distances in the range 4.5–27 km given the typical average distance of 4.5 km covered daily by elephants in the eastern Okavango Panhandle (Vogel et al., 2020; Loarie et al., 2009). The ranges were coupled with the areas defined by the SDEs, and it was estimated that elephants may have walked an average of 16.5 km (±6.2 km) after initial exposure to harmful cyanobacteria blooms and cyanotoxins and could have died within 88 h (±33 h).

3.4. Potential sources of the die-off

A set of 151 pans were identified from the larger pool of 1232 pans spatially associated to carcass cluster centres using a series of thresholds. NDCI = 0.3 was used to indicate higher-than-average phytoplankton biomass in pans. This was obtained by adding the mean and standard deviation of NDCI from all 1232 pans between Aug 2015 and Sep 2023, and pulling the maximum value from the upper standard deviation, noting that the average NDCI across 8 years was 0.2. Additionally, an increase of NDCI = 0.1 between consecutive (bi-weekly) timestamps was arbitrarily used as an indicator of severe bloom events. All 151 pans showed either NDCI >0.3 or NDCI increase of 0.1 units between consecutive timestamps, or both, during the key period Mar-May 2020, when elephants were recorded to have died in large numbers. Surprisingly, all 151 pans fell within the estimated elephants' areas of travel (Table S1), and where only spatially associated to the largest cluster of carcasses (Cluster 1; Fig. 2 C and D). These pans showed repeated high phytoplankton biomass events, with NDCI values up to 0.5. The period

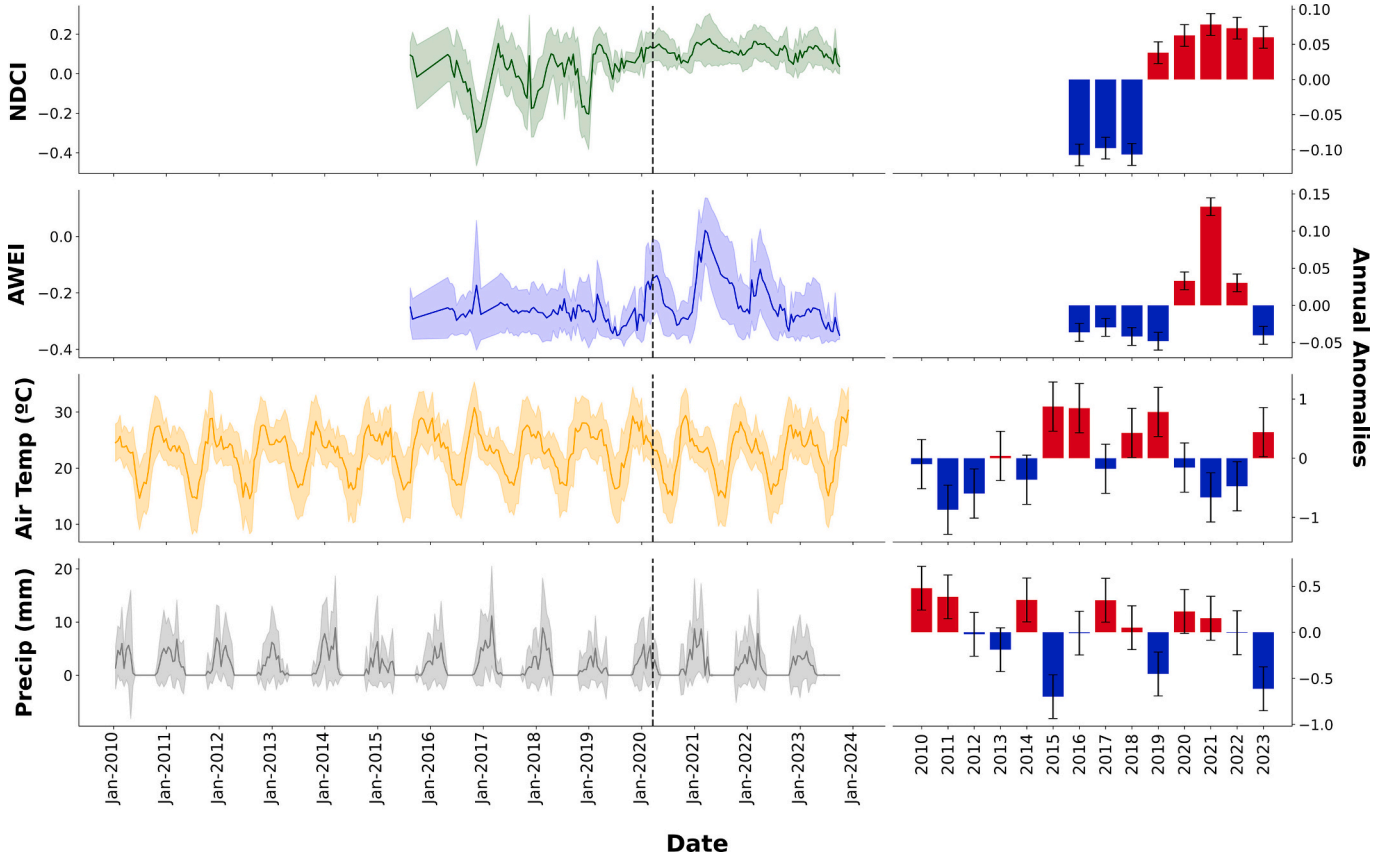

Fig. 3. The four panels on the left show the bi-weekly averages of the Normalised Difference Chlorophyll Index (NDCI), the Automated Water Extraction Index (AWEI), air temperature and precipitation, from top to bottom. The vertical black dotted line aligns with the time of first elephant death reporting (18/03/2020 (African News Agency, 2020)). The four bar plots on the right show the anomalies between the 'long-term' averages of NDCI, AWEI, air temperature, and precipitation, and their annual averages, from top to bottom. The long-term averages for NDCI and AWEI were calculated from the period 2016–2023, limited by Sentinel-2 Multispectral Instrument-A/B observations, which started in August 2015. The long-term averages for air temperature and precipitation were calculated from the period 2010–2023.

Table 2
Table of the timeframes (in hours) of animal death after cyanobacteria exposure found in the literature, with relative number of observations. Animals are listed in order of size (small to large, top to bottom). A summary of cyanobacteria species and cyanotoxin reported (when both available), along with their references are provided (this was only available for dogs and cattle).

Animals	Min (hours)	Max (hours)	Mean (hours)	N Obs.	Cyanotoxin	Cyanobacteria	Reference
Ducks	0.50	2.00	1.25	2			
Geese	0.25	0.50	0.42	3			
Chickens	0.50	2.00	1.50	3			
Turkeys	0.50	2.00	1.00	3			
Dogs	0.25	120.00	18.49	43			
					Anatoxin-a	Anabaena sp.	(Carmichael, 1991)
						Planktothrix sp.	(Puschner et al., 2008)
						Oscillatoria sp.	(Edwards et al., 1992; Gunn et al., 1992)
						Phormidium favosum	(Gugger et al., 2005)
						Lyngbya sp.	(Puschner et al., 2008)
					Microcystin	*Microcystis aeruginosa*	(Johnston and Jacoby, 2003)
					Microcystin-LR	Anabaena sp.	(Walker et al., 2008; Backer et al., 2013)
					Nodularin	*Nodularia spumigena*	(Harding et al., 1995)
						Microcystis aeruginosa	
Sheep	0.50	48.00	11.21	7			
Pigs	0.50	24.00	8.90	5			
Deer	1.00	4.00	2.00	1			
Horses	1.00	24.00	6.33	3			
Cattle	0.25	72.00	21.07	22			
					Cylindrospermopsin	*Cylindrospermopsis raciborskii*	(Thomas et al., 1998; Saker et al., 1999)
					Microcystin	*Microcystis aeruginosa*	(Fitzgerald and Poppenga, 1993)
					Microcystin-LR	Microcystis sp.	(Puschner et al., 1998)
Rhinos	24.00	24.00	24.00	1			

between April and May 2020 showed the highest algae production, although high productivity and bloom events were recorded throughout the year. On average, these pans had water in the period Jan-Jul 2019 only 11 % of the time, compared to 55 % during the same period in 2020.

A smaller set of 20 pans was identified as the most likely candidate sources of poisoning. This group of pans showed repeated bloom events in 2020, recording NDCI increases of 0.1 between consecutive

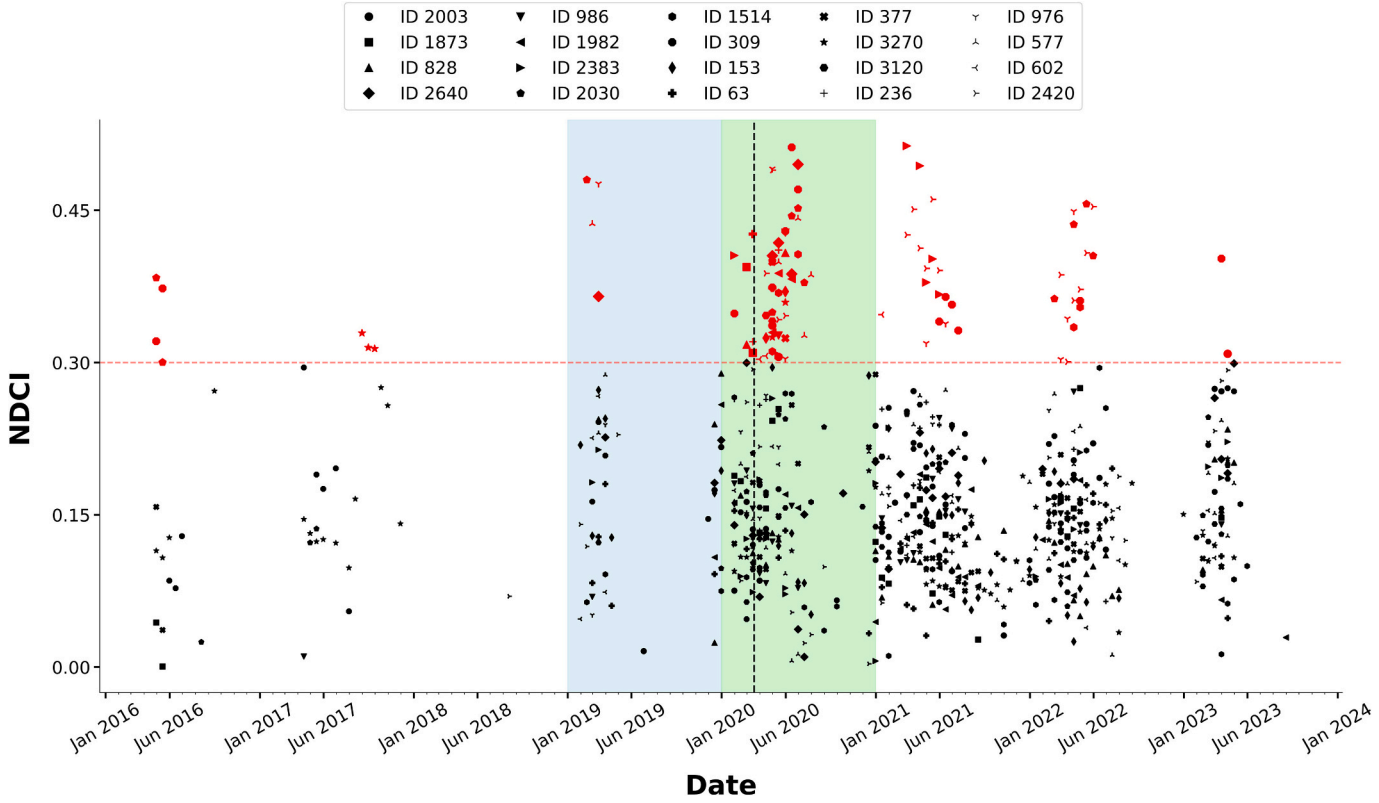

Fig. 4. Timeseries of the twenty pans in eastern Okavango Panhandle that showed the highest algal biomass activity in 2020. Some of the pans show no points prior 2019 because they were likely dry, or too small to be detected using Sentinel-2 Multispectral instrument-A/B images. The horizontal red dotted line is placed on NDCI = 0.3 to show the maximum upper-end NDCI average within the region. Red markers are single observations (pans) when NDCI was >0.3. The vertical black dotted line aligns with the time of first elephant death reporting (18/03/2020 (African News Agency, 2020)). Areas shaded in blue and green correspond to the 12 months in 2019 and 2020, respectively.

timestamps more than twice in the period Mar-May 2020. Satellite observations revealed that this group of pans experienced unprecedented phytoplankton biomass between March and May 2020, and that were either completely dry prior to 2020, or too small to be detected using MSI-A/B images, with a few exceptions (Fig. 4). Visual inspection of SuperDove images at 3 m spatial resolution confirmed that these 20 pans exhibited repeat bloom events between April and May 2020, at different times and intensities (Fig. S2). During this period, the size of these pans ranged between 2 and 22 km^2, demonstrating how bloom events occurred irrespective of size or water availability. SuperDove images also revealed that the landscape surrounding these pans was highly heterogeneous, with no obvious links between land cover types around pans and bloom events. Finally, the average distance of these pans from the centre of Cluster 1 was 11.6 km (±5.2 km), aligning with the estimated distance walked by elephants before dying.

4. Discussion

This study investigated the 2020 elephant die-off event in the eastern Okavango Panhandle in Botswana using an extensive spatial analysis of the carcass locations in concert with a remote sensing assessment of water quality in pans. By comparing the locations of carcasses and elephant bones and linking locations to the ecohydrology of the thousands of pans in the study region we provide new evidence to support the likelihood that deaths may be linked to cyanotoxin poisoning. Our results highlight that seasonal, predominantly rain-fed pans, rather than the permanent waterbodies (i.e., lakes, rivers, and lagoons) within the Panhandle, were the likely source of cyanotoxin exposure. Pans in close proximity to the carcasses showed elevated phytoplankton biomass and repeated bloom events in 2020 compared to previous years, particularly during the period associated with the mass mortality event (Van Aarde et al., 2021), increasing the likelihood of cyanotoxin accumulation in pan water.

Live elephants were mostly found near the Okavango Delta because in the dry month of July they move there for water and to forage (Pozo et al., 2018). Some elephants clustered along the veterinary fence probably because it acts as a physical barrier that prevents them from ranging further (Naidoo et al., 2020). Elephant bones representing deaths in previous years were, in contrast to fresh carcasses, more spread out across the landscape, as demonstrated by the high number of spatial clusters over a wider area (Fig. 2 A), indicative of a weaker spatial relationship between these points. Some points associated with relatively high numbers of individuals were found nearer the Okavango Delta. One likely cause may be mortality from human-elephant conflict, indicated by their proximity to human settlements and the associated increased mortality risk for elephants, owing to high human-elephant competition for shared space and resources in this area of the eastern Okavango Panhandle (Songhurst and Coulson, 2014). Heightened competition for space and resources often leads to problematic animal control mortalities (Songhurst, 2017) and sometimes increases the risk of poaching (Schlossberg et al., 2019). However, predation and natural causes leading to accumulations of bones cannot be ruled out.

Fresh elephant carcasses were predominantly distributed in a region far from the Okavango River and Delta and human settlements. These carcasses were more densely clustered than bones, indicating that the cause of death was likely localised in this area (Fig. 2 C). The higher proximity of fresh carcasses to pans compared to bones may be due to seasonality, since at the time of high elephant mortality in 2020, towards the end of the wet season, elephants tend to stay closer to pans with water (Loarie et al., 2009). The fact that the average distance between carcasses and the nearest pans was lower than bones (Fig. 2 D) could also be linked to an observed altered behaviour of sick elephants roaming closer to water sources (Roever et al., 2013; Haynes, 1988). Nonetheless, this spatial pattern is also consistent with water in pans as the source of any potential cyanotoxin exposure. The additional temporal relationships with phytoplankton biomass, such that clustering of fresh carcasses was associated with specific overgrowth events, provides compelling evidence for a causative link, rather than elephants being drawn to water in general, and in contrast to reporting of algal bloom anomalies in the wider region (Veerman et al., 2022). The strong clustering of carcasses also suggests that the event was sudden, with limited dispersal of elephants prior to death. Notably, a single cluster of carcasses (Cluster 4, Fig. 2 D) was found much further from the others. These elephants may have been part of the same herd, but moved towards this area while sick and their movement was later limited by the standing waters in the Okavango Delta.

Water availability was a major issue in the eastern Okavango Delta in 2019, when it was at its lowest level of the past 8 years (Fig. 3). This was likely driven by lower-than-average precipitation between Oct 2018 and Mar 2019, and higher-than-average temperature in May-Sep 2018. This is particularly relevant for the pans close to the sites of fresh carcasses since these are far from the Okavango Delta and are primarily filled by rain or groundwater, normally recharged by floods, thereby contributing to the observed patterns (Ramberg et al., 2006). Lack of precipitation and higher temperatures have led to the drying of most pans between 2018 and 2019, and long-standing stagnant waters, where available, likely promoted increased phytoplankton activity. Cyanobacteria are frequently abundant in turbid, nutrient-rich waters (Huisman et al., 2018), and tend to dominate these types of water over other phytoplankton species (Paerl and Otten, 2013). We theorise that the shift from such a dry 2019 and an extremely wet 2020 may have led to a resuspension of significant amounts of sediments and nutrients, both from the previously dry beds of the pans and the surrounding soil, promoting unprecedented productivity in 2020.

The process of nutrients release through sediment resuspension is known (Welch and Cooke, 2005), and has been documented for the seasonally dry wetlands of the Okavango Delta (Krah et al., 2006). Pans that were either completely dry or with little water left in 2019 experienced a dramatic volume of water delivered by rainfall, directly exposing them to sediment resuspension and the associated nutrient release. It is important to state that this process does not affect waterbodies equally, even if very similar in principle and surrounded by the same landscape, and that the release of nutrients and consequent eutrophication are system-dependent (Welch and Cooke, 2005). This variability emphasises the need for individual pan analysis in our research, to avoid assuming uniform ecological dynamics across neighbouring pans. Residual cyanotoxins might have persisted in the pans from previous years as shown for deserts' soil crusts (Richer et al., 2015; Cirés et al., 2017; Chatziefthimiou et al., 2021), and there is a possibility that those produced prior to 2020 may have remained in the pans' dried-up bed soil and resuspended in the water. Furthermore, cyanobacteria cells deposited in the sediment from previous years might have inoculated pans' water and increases chances of bloom formation.

Unsurprisingly, April and May were the months with the highest frequency of bloom events in 2020. This period is at the end of the rainy season when rainfall drastically decreases and temperature start rising. Thus, standing water in pans remain relatively undisturbed, presenting the ideal conditions for cyanobacterial growth. The analysis shows that 2015 was also a very dry year (Fig. 3), but the following 2016 rainy season did not deliver the same volumes of water of 2020, which may explain why such sustained phytoplankton biomass levels were not observed then. Although our analysis of water presence and quality in pans is limited to the period 2015–2023, a recent study has shown that 2019 was the driest year of the past two decades in the region (Veerman et al., 2024). The resuspension processes and related nutrient increase in pans we describe, coupled with the unprecedented succession of events between 2019 and 2020, could explain why a mortality event of this size was yet to be recorded in Botswana in the scientific literature.

An understanding of the spatial-temporal dynamics is essential for determining the movement patterns of elephants in response to cyanotoxin exposure. We estimated that elephants may have walked an average of 16.5 km (± 6.2 km) before dying within approximately 88 h

(±33 h) and this aligns with reported toxicological timelines for other large mammals (Wood, 2016). It is worth noting that the approach to establishing the distance walked by elephants before dying is not based on observed elephant movement, since it is challenging to determine movement behaviours from point analysis, and noting that elephants do not move in a single direction throughout the day (Loarie et al., 2009; Vogel et al., 2020). Therefore, the analysis is not intended to inform on walking behaviours of elephants after initial potential exposure to cyanotoxins. Instead, it attempts to estimate the potential distances that elephants may have walked before dying, and possibly the time it may have taken them to die after initial (or repeated) cyanotoxin ingestion based on the distribution of the carcasses.

By analysing bloom dynamics in the pans spatially associated with carcasses cluster centres, we pinpointed 20 locations that experienced extremely frequent and severe bloom events of different magnitudes during the critical period between April and May 2020 (Fig. 4). These pans were all spatially associated to Cluster 1, the cluster with the largest number of individuals (Fig. 2, D), and were all located an average of 11.6 km (±5.2 km) from the centre of the cluster. This figure aligns with the estimated distance walked by elephants before dying, making these pans strong candidates as the potential sources of the intoxication. These pans were of various sizes and surrounded by different types of landscapes (Fig. S2), so it is challenging to determine what may have made them particularly susceptible to bloom events.

Since cyanotoxins are not directly detectable from space, it is not possible to determine which pans contained lethal concentrations and for how long. Nevertheless, prolonged, and repeated algal bloom events increase the likelihood of cyanotoxins in the water, provided the presence of toxin-producing strains of cyanobacteria (Merel et al., 2013), which have been already observed in the African continent, and in particularly high levels in southern African regions (Oberholster et al., 2009; Zhao et al., 2023). Since elephants can drink between 100 and 200 L of water per day, depending on temperatures (Sikes, 1971; Fowler and Mikota, 2006; Dunkin et al., 2013), it is highly likely that they drank from multiple pans before their death. It cannot be established if the fatal intoxication occurred in a single drinking event, but it seem more plausible that if cyanotoxins were present and were the cause of the die-off, this was through toxins bioaccumulation in elephants' organs (Chorus and Welker, 2021).

The recent finding of *Pasteurella* spp. in elephant carcasses in Zimbabwe has shed light on the possibility of African elephants to contract this bacterial infection in Botswana also, although it remains uncertain what may have led to its development and transmission (Foggin et al., 2023). It is possible that elephants in the eastern Okavango Panhandle contracted and spread the disease, leading to the disruption of their immune systems, altered movement, and sensitivity to other mortality factors. Ingestion of higher concentrations, or more potent, cyanotoxins from water compared to 'normal' levels may conversely have led to higher susceptibility to other bacteria, including *Pasteurella* spp., leading to their death. The association between cyanobacterial intoxication and the presence of *Pasteurella multocida*, has previously been reported in a study that found traces of *Pasteurella* in various internal organs of flamingo carcasses arisen from a mortality event in Tanzania (Nonga et al., 2011). This is not an exhaustively comparable study but raises questions on our current understanding of the interplay between cyanobacteria and other bacteria species, including *Pasteurella*.

Unfortunately, we do not have evidence from the ground to corroborate either *Pasteurella* spp., cyanotoxins, or a given species of cyanobacteria, or other diseases as the dominant cause. Our evidence shows that, at the very least, mortality was highly localised near water sources of suspect quality, from currently available remote sensing methods. Future launch of high spatial resolution sensors (order of 1–10 m) equipped with diagnostic wavebands for cyanobacteria pigment (around 620 nm), like those on current medium resolution (300 m) ocean colour sensors, would contribute greatly to diagnosing cyanobacteria dynamics in these ecosystems. Other causes, including poaching, have been previously ruled out (Azeem et al., 2020), and the analysis shows that water was widely available in the eastern Okavango Panhandle in 2020. Hence, death by lack of water (or drought), which has historically led to multiple elephant mass mortality events in Africa (Corfield, 1973; Wato et al., 2016; Ndlovu et al., 2023), does not seem plausible given the presence of water throughout the region at the time of the event.

The drinking behaviour of elephants might have played a role in their susceptibility to cyanotoxins, as drinking depth and timing might impact cyanotoxin intake due to cyanobacterial aggregation influenced by density variations, photosynthetic cycles, and environmental factors (Evans et al., 2000; Gao et al., 2014). This can lead to different toxin concentrations at various water layers, which elephants may be more likely to encounter. Differently from other species that drink from the side of pans, elephants wade into the middle of the waters to drink (Wang et al., 2021), with the potential of disturbing benthic mats (Bouma-Gregson et al., 2018) or causing planktonic biomass to sink and accumulate at the bottom. This behaviour, coupled with the way elephants submerge their trunk to drink, can expose elephants to higher concentrations of cyanotoxins (Wang et al., 2021). Additionally, waterbodies in southern Africa have been observed to frequently hold cyanotoxins concentrations thousands of times higher than WHO guidelines for safe drinking water for humans and animals (Wang et al., 2021; Zhao et al., 2023), further exposing these mammals to extremely dangerous levels of cyanotoxins. While our research primarily focuses on planktonic cyanobacteria, other forms could also contribute to toxicity, highlighting the complexity of these ecosystems.

While elephants may have been more exposed to cyanotoxins due to their drinking behaviour (and the sheer quantity of water they consume daily), it is possible that other species were affected differently due to their drinking habits, which might have led them to ingest smaller quantities of cyanotoxins. The die-off occurred between March and May 2020, and the aerial survey was conducted in July 2020. The time gap between the event and the survey, coupled with the lack of ground-truthing, presents significant challenges in detecting the involvement of other species. Smaller carcasses would have been more susceptible to rapid scavenging and decomposition during this period. The survey might have been less effective in identifying smaller carcasses, especially in areas with dense vegetation. Additionally, high predation risks and the presence of scavengers in the region likely resulted in the quick removal of smaller carcasses (Schiess-Meier et al., 2007; Kesch et al., 2015; Selebatso et al., 2017). The possibility that other species were affected but not detected due to these factors cannot be excluded, and this underscores the need for cautious interpretations.

The southern African region is projected to become drier and hotter (Engelbrecht et al., 2015; Nangombe et al., 2018), and pans across these regions will likely be subject to much shorter hydroperiods (Schaffer-Smith et al., 2022), with potential negative effects on water quantity and quality, and catastrophic repercussions on animals. In this context, the suggested distance covered by the elephants and the time passed after potential exposure to cyanotoxins not only shed light on this specific event but also represents the first steps in establishing a framework for investigating future mortality events of unknown causes in large mammals. This framework could be particularly crucial in regions experiencing drastic environmental changes. More efforts to improve mapping and further characterise pan ecohydrology are fundamental to understanding the implications of climate change on the ecology of the Okavango and other important ecosystems in the region, and beyond. We believe that the methods and findings of this study may serve future management and conservation strategies, providing a basis for addressing the challenges posed by changing environmental conditions. Integrating spatial analysis techniques in animal surveying could further serve as an early warning system to capture the onset and origin of animal mortality events, thereby offering a proactive approach to conservation. Developing a concurrent efficient sampling protocol that can

be mobilised in response to or during these climatic and ecohydrological changes would add significant impact to early warning monitoring and management response strategies.

In conclusion, this unprecedented die-off within the largest remaining population of a threatened signature megafauna underlines the escalating concerns surrounding the impact of drought and climate change on the Okavango Delta, one of the most important ecosystems in the world. Globally, this event underscores the alarming trend of sudden, climate-induced diseases affecting large ungulates, reflecting the broader, devastating impacts of climate change on biodiversity and ecosystem health (Kutz et al., 2015; Kock et al., 2018). By establishing a methodological approach to tracking and analysing these events, our study contributes to the broader field of environmental science and animal conservation, providing critical insights that could help mitigate similar tragedies in the future.

CRediT authorship contribution statement

Davide Lomeo: Writing – review & editing, Writing – original draft, Visualization, Methodology, Investigation, Formal analysis, Conceptualization. **Emma J. Tebbs:** Writing – review & editing, Supervision, Methodology, Investigation, Conceptualization. **Nlingisisi D. Babayani:** Writing – review & editing, Investigation. **Michael A. Chadwick:** Writing – review & editing, Investigation. **Mangaliso J. Gondwe:** Writing – review & editing, Investigation. **Anne D. Jungblut:** Writing – review & editing, Supervision. **Graham P. McCulloch:** Writing – review & editing. **Eric R. Morgan:** Writing – review & editing, Data curation. **Daniel N. Schillereff:** Writing – review & editing, Supervision. **Stefan G.H. Simis:** Writing – review & editing, Supervision. **Anna C. Songhurst:** Writing – review & editing, Data curation.

Declaration of competing interest

The authors declare that they have no known competing financial interests or personal relationships that could have appeared to influence the work reported in this paper.

Acknowledgments

We would like to thank the Government of Botswana Ministry of Environment, Nature Conservation and Tourism, Ministry of Agriculture, Department of Wildlife and National Parks, and Department of Veterinary Services for granting permission for this research to take place, as well as providing data and resources. Thank you to all the team members involved in the research. Thank you to Natural Environmental Research Council (NERC) for providing funding for this research through Urgency grant NE/V013114/1, and the London NERC DTP grant NE/S007229/1, and thank you to the Elephant Crisis Fund, DWNP and Ecoexist for co-funding the elephant population survey. For the purpose of open access, the author has applied a Creative Commons Attribution (CC BY) license to any Author Accepted Manuscript version arising.

Appendix A. Supplementary data

Supplementary data to this article can be found online at https://doi.org/10.1016/j.scitotenv.2024.177525.

Data availability

Data was collected and analysed with permission of the Republic of Botswana Ministry of Environment, Nature Conservation and Tourism, research permit ENT 8/36/4 XLIX (11) and Ministry of Agriculture, research permit DVS 8/2/II (28).

The elephant survey data used in this study cannot be deposited in a public repository because it is owned by Ecoexist (https://www.ecoexistproject.org). To request access, contact info@ecoexistproject.org. Satellite data was obtained from Google Earth Engine, and available to those that sign up to the service (https://code.earthengine.google.com).

Any additional information required to analyse the data reported in this paper, including the code, is available from the lead contact upon request.

References

African News Agency, 2020. *Botswana probes mysterious death of 56 elephants*. 2020. https://www.iol.co.za/news/africa/botswana-probes-mysterious-death-of-56-elephants-48239310 [Accessed: 19 December 2023].

Akinyemi, F.O., Abiodun, B.J., 2019. Potential impacts of global warming levels 1.5 °C and above on climate extremes in Botswana. Clim. Chang. 154 (3–4), 387–400. https://doi.org/10.1007/s10584-019-02446-1.

Anselin, L., 1995. Local Indicators of Spatial Association-LISA. Geogr. Anal. 27 (2), 93–115. https://doi.org/10.1111/j.1538-4632.1995.tb00338.x.

Azeem, S., Bengis, R., Van Aarde, R., Bastos, A.D.S., 2020. Mass die-off of African elephants in Botswana: pathogen, poison or a perfect storm? Afr. J. Wildl. Res. 50 (1). https://doi.org/10.3957/056.050.0149.

Backer, L., Landsberg, J., Miller, M., Keel, K., Taylor, T., 2013. Canine cyanotoxin poisonings in the United States (1920s–2012): review of suspected and confirmed cases from three data sources. Toxins 5 (9), 1597–1628. https://doi.org/10.3390/toxins5091597.

Barton, P.S., Reboldi, A., Bonat, S., Mateo-Tomás, P., Newsome, T.M., 2023. Climate-driven animal mass mortality events: is there a role for scavengers? Environ. Conserv. 50 (1), 1–6. https://doi.org/10.1017/S0376892922000388.

Bengis, R., Govender, D., Lane, E., Myburgh, J., Oberholster, P., Buss, P., Prozesky, L., Keet, D., 2016. Eco-epidemiological and pathological features of wildlife mortality events related to cyanobacterial bio-intoxication in the Kruger National Park, South Africa. J. S. Afr. Vet. Assoc. 87 (1). https://doi.org/10.4102/jsava.v87i1.1391.

Benza, B., 2020. Botswana says toxins in water killed hundreds of elephants. 2020. https://www.reuters.com/article/us-botswana-elephants-idUSKCN26C0WA/. (Accessed 20 November 2023).

Bouma-Gregson, K., Kudela, R.M., Power, M.E., 2018. Widespread anatoxin-a detection in benthic cyanobacterial mats throughout a river network J.-F. Humbert (ed.). PLoS One 13 (5), e0197669. https://doi.org/10.1371/journal.pone.0197669.

Braaten, J., 2023. *Sentinel-2 cloud masking with s2cloudless*. 2023. https://developers.google.com/earth-engine/tutorials/community/sentinel-2-s2cloudless. (Accessed 20 August 2023).

Bussière, E.M.S., Potgieter, D., 2023. KAZA Elephant Survey 2022. Volume I, Results and Technical Report, KAZA TFCA Secretariat, Kasane, Botswana. https://www.wwf.de/fileadmin/fm-wwf/Publikationen-PDF/Afrika/KAZA-Elephant-Survey-Volume-1.pdf.

Byakatonda, J., Parida, B.P., Kenabatho, P.K., 2018. Relating the dynamics of climatological and hydrological droughts in semiarid Botswana. Phys. Chem. Earth, Parts A/B/C. 105, 12–24. https://doi.org/10.1016/j.pce.2018.02.004.

Carmichael, W., 1991. Blue-green algae: an overlooked health threat. Health Environ. Digest. 5 (6), 1–4.

Chase, M., Schlossberg, S., Sutcliffe, R., Seonyatseng, E., 2018. Dry season aerial survey of elephants and wildlife in Northern Botswana. https://elephantswithoutborders.org/site/wp-content/uploads/2018-Botswana-report-final-version-compressed-upload.pdf.

Chatziefthimiou, A.D., Banack, S.A., Cox, P.A., 2021. Biocrust-produced cyanotoxins are found vertically in the desert soil profile. Neurotox. Res. 39 (1), 42–48. https://doi.org/10.1007/s12640-020-00224-x.

Chorus, I., Welker, M., 2021. Toxic cyanobacteria in Water: A Guide to their Public Health Consequences, Monitoring and Management, Second edition. CRC Press, Boca Raton London New York.

Cirés, S., Casero, M., Quesada, A., 2017. Toxicity at the edge of life: a review on cyanobacterial toxins from extreme environments. Mar. Drugs 15 (7), 233. https://doi.org/10.3390/md15070233.

Clark, P.J., Evans, F.C., 1954. Distance to nearest neighbor as a measure of spatial relationships in populations. Ecology 35 (4), 445–453. https://doi.org/10.2307/1931034.

Corfield, T.F., 1973. Elephant mortality in Tsavo National Park, Kenya. Afr. J. Ecol. 11 (3–4), 339–368. https://doi.org/10.1111/j.1365-2028.1973.tb00098.x.

CREODIAS, 2023. CREODIAS. 2023. https://explore.creodias.eu. (Accessed 20 August 2023).

Dalu, T., Wasserman, R.J., 2018. Cyanobacteria dynamics in a small tropical reservoir: understanding spatio-temporal variability and influence of environmental variables. Sci. Total Environ. 643, 835–841. https://doi.org/10.1016/j.scitotenv.2018.06.256.

Douglas-Hamilton, I., Burrill, A., 1991. Using Elephant Carcass Ratios to Determine Population Trends. Research and Management, African Wildlife, pp. 98–105.

Dunkin, R.C., Wilson, D., Way, N., Johnson, K., Williams, T.M., 2013. Climate influences thermal balance and water use in African and Asian elephants: physiology can predict drivers of elephant distribution. J. Exp. Biol. 216 (15), 2939–2952. https://doi.org/10.1242/jeb.080218.

Ecoexist, 2023. THE ECOEXIST PROJECT: reducing conflict and fostering coexistence between elephants and people. 2023. https://www.ecoexistproject.org. (Accessed 5 December 2023).

Edwards, C., Beattie, K.A., Scrimgeour, C.M., Codd, G.A., 1992. Identification of anatoxin-a in benthic cyanobacteria (blue-green algae) and in associated dog poisonings at Loch Insh, Scotland. Toxicon 30 (10), 1165–1175. https://doi.org/10.1016/0041-0101(92)90432-5.

Engelbrecht, F., Adegoke, J., Bopape, M.-J., Naidoo, M., Garland, R., Thatcher, M., McGregor, J., Katzfey, J., Werner, M., Ichoku, C., Gatebe, C., 2015. Projections of rapidly rising surface temperatures over Africa under low mitigation. Environ. Res. Lett. 10 (8), 085004. https://doi.org/10.1088/1748-9326/10/8/085004.

ESA, 2020a. Sen2Cor Software Release Note. http://step.esa.int/thirdparties/sen2cor/2.9.0/docs/S2-PDGS-MPC-L2A-SRN-V2.9.0.pdf.

ESA, 2020b. *Sen2Cor v2.9*. 2020. https://step.esa.int/main/snap-supported-plugins/sen2cor/sen2cor-v2-9/ [Accessed: 20 August 2023].

Ester, M., Kriegel, H.-P., Xu, X., 1996. A density-based algorithm for discovering clusters in large spatial databases with noise. KDD-96 Proc. 226–231.

Evans, A.M., Gallon, J.R., Jones, A., Staal, M., Stal, L.J., Villbrandt, M., Walton, T.J., 2000. Nitrogen fixation by Baltic cyanobacteria is adapted to the prevailing photon flux density. New Phytol. 147 (2), 285–297. https://doi.org/10.1046/j.1469-8137.2000.00696.x.

Feng, L., Wang, Y., Hou, X., Qin, B., Kuster, T., Qu, F., Chen, N., Paerl, H.W., Zheng, C., 2024. Harmful algal blooms in inland waters. Nat. Rev. Earth Environ. https://doi.org/10.1038/s43017-024-00578-2.

Feyisa, G.L., Meilby, H., Fensholt, R., Proud, S.R., 2014. Automated Water Extraction Index: a new technique for surface water mapping using Landsat imagery. Remote Sens. Environ. 140, 23–35. https://doi.org/10.1016/j.rse.2013.08.029.

Fitzgerald, S.D., Poppenga, R.H., 1993. Toxicosis due to Microcystin Hepatotoxins in Three Holstein Heifers. J. Vet. Diagn. Invest. 5 (4), 651–653. https://doi.org/10.1177/104063879300500433.

Foggin, C.M., Rosen, L.E., Henton, M.M., Buys, A., Floyd, T., Turner, A.D., Tarbin, J., Lloyd, A.S., Chaitezvi, C., Ellis, R.J., Roberts, H.C., Dastjerdi, A., Nunez, A., Van Vliet, A.H.M., Steinbach, F., 2023. Pasteurella sp. associated with fatal septicaemia in six African elephants. Nat. Commun. 14 (1), 6398. https://doi.org/10.1038/s41467-023-41987-z.

Fowler, M.E., Mikota, S.K., 2006. Biology, Medicine, and Surgery of Elephants, 1st edition. Wiley. https://doi.org/10.1002/9780470344484.

Gao, Y., O'Neil, J., Stoecker, D., Cornwell, J., 2014. Photosynthesis and nitrogen fixation during cyanobacteria blooms in an oligohaline and tidal freshwater estuary. Aquat. Microb. Ecol. 72 (2), 127–142. https://doi.org/10.3354/ame01692.

Gugger, M., Lenoir, S., Berger, C., Ledreux, A., Druart, J.-C., Humbert, J.-F., Guette, C., Bernard, C., 2005. First report in a river in France of the benthic cyanobacterium Phormidium favosum producing anatoxin-a associated with dog neurotoxicosis. Toxicon 45 (7), 919–928. https://doi.org/10.1016/j.toxicon.2005.02.031.

Gunn, G., Rafferty, A., Rafferty, G., Cockburn, N., Edwards, C., Beattie, K., Codd, G., 1992. Fatal canine neurotoxicosis attributed to blue-green algae (cyanobacteria). Vet. Rec. 130 (14), 301–302. https://doi.org/10.1136/vr.130.14.301.

Harding, W.R., Rowe, N., Wessels, J.C., Beattie, K.A., Codd, G.A., 1995. Death of a dog attributed to the cyanobacterial (blue-green algal) hepatotoxin nodularin in South Africa. J. S. Afr. Vet. Assoc. 66 (4), 256–259.

Hart, R.C., 1997. A limnological profile of the upper Okavango Delta at low water level. South. Afr. J. Aquat. Sci. 23 (2), 21–33. https://doi.org/10.1080/10183469.1997.9631398.

Haynes, G., 1988. Longitudinal studies of african elephant death and bone deposits. J. Archaeol. Sci. 15 (2), 131–157. https://doi.org/10.1016/0305-4403(88)90003-9.

Hersbach, H., Bell, B., Berrisford, P., Horányi, A., Muñoz Sabater, J., Nicolas, J., Peubey, C., Radu, R., Rozum, I., Schepers, D., Simmons, A., Soci, C., Dee, D., Thépaut, J.-N., 2023. ERA5 hourly data on single levels from 1940 to present. In: Copernicus Climate Change Service (C3S) Climate Data Store (CDS). https://doi.org/10.24381/cds.adbb2d47.

Hou, X., Feng, L., Dai, Y., Hu, C., Gibson, L., Tang, J., Lee, Z., Wang, Y., Cai, X., Liu, J., Zheng, Y., Zheng, C., 2022. Global mapping reveals increase in lacustrine algal blooms over the past decade. Nat. Geosci. 15 (2), 130–134. https://doi.org/10.1038/s41561-021-00887-x.

Huisman, J., Codd, G.A., Paerl, H.W., Ibelings, B.W., Verspagen, J.M.H., Visser, P.M., 2018. Cyanobacterial blooms. Nat. Rev. Microbiol. 16 (8), 471–483. https://doi.org/10.1038/s41579-018-0040-1.

Johnston, B.R., Jacoby, J.M., 2003. Cyanobacterial toxicity and migration in a mesotrophic lake in western Washington, USA. Hydrobiologia 495, 79–91.

Kesch, M.K., Bauer, D.T., Loveridge, A.J., 2015. Break on through to the other side: the effectiveness of game fencing to mitigate human—wildlife conflict. Afr. J. Wildl. Res. 45 (1), 76. https://doi.org/10.3957/056.045.0109.

Kock, R.A., Orynbayev, M., Robinson, S., Zuther, S., Singh, N.J., Beauvais, W., Morgan, E. R., Kerimbayev, A., Khomenko, S., Martineau, H.M., Rystaeva, R., Omarova, Z., Wolfs, S., Hawotte, F., Radoux, J., Milner-Gulland, E.J., 2018. Saigas on the brink: multidisciplinary analysis of the factors influencing mass mortality events. Sci. Adv. 4 (1), eaao2314. https://doi.org/10.1126/sciadv.aao2314.

Krah, M., McCarthy, T.S., Huntsman-Mapila, P., Wolski, P., Annegarn, H., Sethebe, K., 2006. Nutrient budget in the seasonal wetland of the Okavango Delta, Botswana. Wetl. Ecol. Manag. 14 (3), 253–267. https://doi.org/10.1007/s11273-005-1115-0.

Kroese, D.P., Brereton, T., Taimre, T., Botev, Z.I., 2014. Why the Monte Carlo method is so important today. WIREs Comput. Stat. 6 (6), 386–392. https://doi.org/10.1002/wics.1314.

Kutz, S., Bollinger, T., Branigan, M., Checkley, S., Davison, T., Dumond, M., Elkin, B., Forde, T., Hutchins, W., Niptanatiak, A., Orsel, K., 2015. Erysipelothrix rhusiopathiae associated with recent widespread muskox mortalities in the Canadian Arctic. Canad. Vet. J. 56 (6), 560–563.

Loarie, S.R., Aarde, R.J.V., Pimm, S.L., 2009. Fences and artificial water affect African savannah elephant movement patterns. Biol. Conserv. 142 (12), 3086–3098. https://doi.org/10.1016/j.biocon.2009.08.008.

Lopes, R.H.C., Reid, I., Hobson, P.R., 2007. The Two-dimensional Kolmogorov-Smirnov Test.

Maidment, R.I., Grimes, D., Allan, R.P., Tarnavsky, E., Stringer, M., Hewison, T., Roebeling, R., Black, E., 2014. The 30 year TAMSAT African Rainfall Climatology And Time series (TARCAT) data set. J. Geophys. Res. Atmos. 119 (18). https://doi.org/10.1002/2014JD021927.

Maidment, R.I., Grimes, D., Black, E., Tarnavsky, E., Young, M., Greatrex, H., Allan, R.P., Stein, T., Nkonde, E., Senkunda, S., Alcántara, E.M.U., 2017. A new, long-term daily satellite-based rainfall dataset for operational monitoring in Africa. Sci. Data 4 (1), 170063. https://doi.org/10.1038/sdata.2017.63.

Marobela-Raborokgwe, C., 2011. Contagious bovine pleuropneumonia in Botswana: experience with control, eradication, prevention and surveillance. Vet. Ital. 47 (4), 397–405.

Maron, D.F., 2020. What's killing Botswana's elephants? Here are the top theories. 2020. https://www.nationalgeographic.com/animals/article/botswana-elephant-death-mystery. (Accessed 20 November 2023).

Massey, F.J., 1951. The Kolmogorov-Smirnov test for goodness of fit. J. Am. Stat. Assoc. 46 (253), 68–78. https://doi.org/10.1080/01621459.1951.10500769.

Matthews, M.W., Bernard, S., Winter, K., 2010. Remote sensing of cyanobacteria-dominant algal blooms and water quality parameters in Zeekoevlei, a small hypertrophic lake, using MERIS. Remote Sens. Environ. 114 (9), 2070–2087. https://doi.org/10.1016/j.rse.2010.04.013.

Merel, S., Walker, D., Chicana, R., Snyder, S., Baurès, E., Thomas, O., 2013. State of knowledge and concerns on cyanobacterial blooms and cyanotoxins. Environ. Int. 59, 303–327. https://doi.org/10.1016/j.envint.2013.06.013.

Mishra, S., Mishra, D.R., 2012. Normalized difference chlorophyll index: a novel model for remote estimation of chlorophyll-a concentration in turbid productive waters. Remote Sens. Environ. 117, 394–406. https://doi.org/10.1016/j.rse.2011.10.016.

Msiteli-Shumba, S., Kativu, S., Utete, B., Makuwe, E., Hulot, F.D., 2018. Driving factors of temporary and permanent shallow lakes in and around Hwange National Park, Zimbabwe. Water SA 44 (2 April). https://doi.org/10.4314/wsa.v44i2.12.

Naidoo, R., Brennan, A., Shapiro, A.C., Beytell, P., Aschenborn, O., Du Preez, P., Kilian, J. W., Stuart-Hill, G., Taylor, R.D., 2020. Mapping and assessing the impact of small-scale ephemeral water sources on wildlife in an African seasonal savannah. Ecol. Appl. 30 (8). https://doi.org/10.1002/eap.2203.

Nangombe, S., Zhou, T., Zhang, W., Wu, B., Hu, S., Zou, L., Li, D., 2018. Record-breaking climate extremes in Africa under stabilized 1.5 °C and 2 °C global warming scenarios. Nat. Clim. Chang. 8 (5), 375–380. https://doi.org/10.1038/s41558-018-0145-6.

Ndlovu, M., Madiri, T.H., Madhlamoto, D., Tadyanehondo, K.M., Vambe, A., Mungoni, E., 2023. Age-sex structure of drought-driven African elephant (Loxodonta africana) mortality in Hwange National Park, Zimbabwe. Sci. Afr. 19, e01459. https://doi.org/10.1016/j.sciaf.2022.e01459.

Nkemelang, T., New, M., Zaroug, M., 2018. Temperature and precipitation extremes under current, 1.5 °C and 2.0 °C global warming above pre-industrial levels over Botswana, and implications for climate change vulnerability. Environ. Res. Lett. 13 (6), 065016. https://doi.org/10.1088/1748-9326/aac2f8.

Nonga, H.E., Sandvik, M., Miles, C.O., Lie, E., Mdegela, R.H., Mwamengele, G.L., Semuguruka, W.D., Skaare, J.U., 2011. Possible involvement of microcystins in the unexplained mass mortalities of Lesser Flamingo (Phoeniconaias minor Geoffroy) at Lake Manyara in Tanzania. Hydrobiologia 678 (1), 167–178. https://doi.org/10.1007/s10750-011-0844-8.

Norton-Griffiths, M., 1978. Counting animals J.J.R. Grimsdell (ed.). https://www.awf.org/sites/default/files/media/Resources/Books%2520and%2520Papers/AWF_1_counting_animals.pdf.

Oberholster, P.J., Botha, A.M., Botha, J.G., 2009. Linking climate change and progressive eutrophication to incidents of clustered animal mortalities in different geographical regions of South Africa. Afr. J. Biotechnol. 8 (21), 5825–5832. https://doi.org/10.5897/AJB09.1060.

Otsu, N., 1979. A threshold selection method from gray-level histograms. IEEE Trans. Syst. Man Cybern. 9 (1), 62–66. https://doi.org/10.1109/TSMC.1979.4310076.

Paerl, H.W., Otten, T.G., 2013. Harmful cyanobacterial blooms: causes, consequences, and controls. Microb. Ecol. 65 (4), 995–1010. https://doi.org/10.1007/s00248-012-0159-y.

Perkins, J.S., 2019. 'Only connect': restoring resilience in the Kalahari ecosystem. J. Environ. Manag. 249, 109420. https://doi.org/10.1016/j.jenvman.2019.109420.

Pozo, R.A., Coulson, T., McCulloch, G., Stronza, A.L., Songhurst, A.C., 2017. Determining baselines for human-elephant conflict: a matter of time S.C. Banks (ed.). PLoS One 12 (6), e0178840. https://doi.org/10.1371/journal.pone.0178840.

Pozo, R.A., Cusack, J.J., McCulloch, G., Stronza, A., Songhurst, A., Coulson, T., 2018. Elephant space-use is not a good predictor of crop-damage. Biol. Conserv. 228, 241–251. https://doi.org/10.1016/j.biocon.2018.10.031.

Puschner, B., Galey, F.D., Johnson, B., Dickie, C.W., Vondy, M., Francis, T., Holstege, D. M., 1998. Blue-green algae toxicosis in cattle. J. Am. Vet. Med. Assoc. 213 (11), 1605–1607 (1571).

Puschner, B., Hoff, B., Tor, E.R., 2008. Diagnosis of Anatoxin-a poisoning in dogs from North America. J. Vet. Diagn. Invest. 20 (1), 89–92. https://doi.org/10.1177/104063870802000119.

Ramberg, L., Wolski, P., Krah, M., 2006. Water balance and infiltration in a seasonal floodplain in the Okavango Delta, Botswana. Wetlands 26 (3), 677–690. https://doi.org/10.1672/0277-5212(2006)26[677:WBAIIA]2.0.CO;2.

Richer, R., Banack, S.A., Metcalf, J.S., Cox, P.A., 2015. The persistence of cyanobacterial toxins in desert soils. J. Arid Environ. 112, 134–139. https://doi.org/10.1016/j.jaridenv.2014.01.023.

Roever, C.L., Van Aarde, R.J., Chase, M.J., 2013. Incorporating mortality into habitat selection to identify secure and risky habitats for savannah elephants. Biol. Conserv. 164, 98–106. https://doi.org/10.1016/j.biocon.2013.04.006.

Saker, M.L., Thomas, A.D., Norton, J.H., 1999. Cattle mortality attributed to the toxic cyanobacteriumCylindrospermopsis raciborskii in an outback region of North Queensland. Environ. Toxicol. 14 (1), 179–182. https://doi.org/10.1002/(SICI)1522-7278(199902)14:1<179::AID-TOX23>3.0.CO;2-G.

Schaffer-Smith, D., Swift, M., Killea, A., Brennan, A., Naidoo, R., Swenson, J.J., 2022. Tracking a blue wave of ephemeral water across arid southern Africa. Environ. Res. Lett. 17 (11), 114063. https://doi.org/10.1088/1748-9326/ac98d9.

Schiess-Meier, M., Ramsauer, S., Gabanapelo, T., König, B., 2007. Livestock predation—insights from problem animal control registers in Botswana. J. Wildl. Manag. 71 (4), 1267–1274. https://doi.org/10.2193/2006-177.

Schlossberg, S., Chase, M.J., Sutcliffe, R., 2019. Evidence of a growing elephant poaching problem in Botswana. Curr. Biol. 29 (13), 2222–2228.e4. https://doi.org/10.1016/j.cub.2019.05.061.

Selebatso, M., Fynn, R., Maude, G., 2017. Adaptive activity patterns of a blue wildebeest population to environmental variability in fragmented, semi-arid Kalahari, Botswana. J. Arid Environ. 136, 15–18. https://doi.org/10.1016/j.jaridenv.2016.10.001.

Sikes, S.K., 1971. The Natural History of the African Elephant. The World naturalist. Weidenfeld & Nicolson, London.

Songhurst, A., 2017. Measuring human–wildlife conflicts: comparing insights from different monitoring approaches. Wildl. Soc. Bull. 41 (2), 351–361. https://doi.org/10.1002/wsb.773.

Songhurst, A., Coulson, T., 2014. Exploring the effects of spatial autocorrelation when identifying key drivers of wildlife crop-raiding. Ecol. Evol. 4 (5), 582–593. https://doi.org/10.1002/ece3.837.

Songhurst, A., Tsholofelo, C., 2020. Elephant Population and Carcass Survey Report. Okavango Panhandle, Botswana (NG10, NG11, NG12 and NG13).p.38.

Songhurst, A., Chase, M., Coulson, T., 2015. Using simulations of past and present elephant (Loxodonta africana) population numbers in the Okavango Delta Panhandle, Botswana to improve future population estimates. Wetl. Ecol. Manag. 23 (4), 583–602. https://doi.org/10.1007/s11273-015-9440-4.

Svirčev, Z., Lalić, D., Bojadžija Savić, G., Tokodi, N., Drobac Backović, D., Chen, L., Meriluoto, J., Codd, G.A., 2019. Global geographical and historical overview of cyanotoxin distribution and cyanobacterial poisonings. Arch. Toxicol. 93 (9), 2429–2481. https://doi.org/10.1007/s00204-019-02524-4.

Swift, M., Schaffer-Smith, D., Killea, A., 2022. Map of surface water frequency observed 2017–2020. In: Schaffer-Smith et al 2022. https://doi.org/10.4211/hs.6f5b34803dc247e890925d7f26b04a3b.

Tarnavsky, E., Grimes, D., Maidment, R., Black, E., Allan, R.P., Stringer, M., Chadwick, R., Kayitakire, F., 2014. Extension of the TAMSAT Satellite-Based Rainfall Monitoring over Africa and from 1983 to Present. JOURNAL OF APPLIED METEOROLOGY AND CLIMATOLOGY. 53.

Thomas, A., Saker, M., Norton, J., Olsen, R., 1998. Cyanobacterium Cylindro-spermopsis raciborskii as a probable cause of death in cattle in northern Queensland. Aust. Vet. J. 76 (9), 592–594. https://doi.org/10.1111/j.1751-0813.1998.tb10233.x.

Van Aarde, R.J., Pimm, S.L., Guldemond, R., Huang, R., Maré, C., 2021. The 2020 elephant die-off in Botswana. PeerJ 9, e10686. https://doi.org/10.7717/peerj.10686.

Veerman, J., Kumar, A., Mishra, D.R., 2022. Exceptional landscape-wide cyanobacteria bloom in Okavango Delta, Botswana in 2020 coincided with a mass elephant die-off event. Harmful Algae 111, 102145. https://doi.org/10.1016/j.hal.2021.102145.

Veerman, J., Mishra, D.R., Kumar, A., Karidozo, M., 2024. Environmental drivers behind the exceptional increase in cyanobacterial blooms in Okavango Delta, Botswana. Harmful Algae 137, 102677. https://doi.org/10.1016/j.hal.2024.102677.

Vogel, S.M., Lambert, B., Songhurst, A.C., McCulloch, G.P., Stronza, A.L., Coulson, T., 2020. Exploring movement decisions: can Bayesian movement-state models explain crop consumption behaviour in elephants (*Loxodonta africana*)? L. Börger (ed.). J. Anim. Ecol. 89 (4), 1055–1068. https://doi.org/10.1111/1365-2656.13177.

Walker, S., Lund, J., Schumacher, D., Brakhage, P., McManus, B., Miller, J., Augustine, M., Carney, J., Holland, R., Hoagland, K., Holz, J., Barrow, T., Rundquist, D., Gitelson, A., 2008. Cyanobacterial harmful algal blooms: state of the science and research needs. In: Hudnell, H.K. (Ed.), Nebraska Experience. Advances in Experimental Medicine and Biology. Springer New York, New York, NY, pp. 139–152. https://doi.org/10.1007/978-0-387-75865-7_6.

Wang, B., Shi, W., Miao, Z., 2015. Confidence analysis of standard deviational ellipse and its extension into higher dimensional Euclidean space D. Rocchini (ed.). PLoS One 10 (3), e0118537. https://doi.org/10.1371/journal.pone.0118537.

Wang, H., Xu, C., Liu, Y., Jeppesen, E., Svenning, J.-C., Wu, J., Zhang, W., Zhou, T., Wang, P., Nangombe, S., Ma, J., Duan, H., Fang, J., Xie, P., 2021. From unusual suspect to serial killer: cyanotoxins boosted by climate change may jeopardize megafauna. The Innovation 2 (2), 100092. https://doi.org/10.1016/j.xinn.2021.100092.

Wato, Y.A., Heitkönig, I.M.A., Van Wieren, S.E., Wahungu, G., Prins, H.H.T., Van Langevelde, F., 2016. Prolonged drought results in starvation of African elephant (Loxodonta africana). Biol. Conserv. 203, 89–96. https://doi.org/10.1016/j.biocon.2016.09.007.

Welch, E.B., Cooke, G.D., 2005. Internal phosphorus loading in shallow lakes: importance and control. Lake Reserv. Manag. 21 (2), 209–217. https://doi.org/10.1080/07438140509354430.

Wood, R., 2016. Acute animal and human poisonings from cyanotoxin exposure — a review of the literature. Environ. Int. 91, 276–282. https://doi.org/10.1016/j.envint.2016.02.026.

Zhao, X., Liu, Y., Guo, Y.-M., Xu, C., Chen, L., Codd, G.A., Chen, J., Wang, Y., Wang, P.-Z., Yang, L.-W., Zhou, L., Li, Y., Xiao, S.-M., Wang, H.-J., Paerl, H.W., Jeppesen, E., Xie, P., 2023. Meta-analysis reveals cyanotoxins risk across African inland waters. J. Hazard. Mater. 451, 131160. https://doi.org/10.1016/j.jhazmat.2023.131160.